

23. D. Mann, thesis, Stanford University (2006).
 24. W. J. Liang *et al.*, *Nature* **411**, 665 (2001).
 25. P. Jarillo-Herrero *et al.*, *Phys. Rev. Lett.* **94**, 156802 (2005).
 26. W. Chen, A. V. Andreev, A. M. Tselik, D. Orgad, *Phys. Rev. Lett.* **101**, 246802 (2008).
 27. S. R. White, I. Affleck, D. J. Scalapino, *Phys. Rev. B* **65**, 165122 (2002).
 28. Because of the sensitivity of the exponent on the model used and the general difficulty of accurately estimating it, the agreement to theory may be somewhat fortuitous. For example, a recent study gives an alternative scaling exponent of $a = 2$ for the gap (26). Nevertheless, our data are described both quantitatively and qualitatively by the theoretical calculations of (10), and the exponent of 1.3 is within the range $a = 1 - 2$ of theoretically predicted values for all the theoretical works cited that include long-ranged Coulomb interactions (10–12, 26).
 29. S. De Franceschi *et al.*, *Phys. Rev. Lett.* **86**, 878 (2001).
 30. L. S. Levitov, A. M. Tselik, *Phys. Rev. Lett.* **90**, 016401 (2003).
 31. M. Garst, D. S. Novikov, A. Stern, L. I. Glazman, *Phys. Rev. B* **77**, 035128 (2008).
 32. We acknowledge Micro Nano Laboratory at Caltech and Nanotech at the University of California, Santa Barbara where fabrication was performed. We thank A. Andreev,

D. Cobden, M. Garst, L. Glazman, S. Ilani, P. King, K. Le Hur, L. Levitov, G. Refael, and G. Steele for helpful discussions. M.B. and V.V.D. acknowledge the support of the Office of Naval Research, the Sloan Foundation, and the Ross Brown. D.N. was supported by NSF grants DMR-0749220 and DMR-0754613.

Supporting Online Material

www.sciencemag.org/cgi/content/full/323/5910/106/DC1
 Fig. S1

11 September 2008; accepted 20 November 2008
 10.1126/science.1165799

Broadband Invisibility by Non-Euclidean Cloaking

Ulf Leonhardt^{1,2*} and Tomáš Tyc^{2,3}

Invisibility and negative refraction are both applications of transformation optics where the material of a device performs a coordinate transformation for electromagnetic fields. The device creates the illusion that light propagates through empty flat space, whereas in physical space, light is bent around a hidden interior or seems to run backward in space or time. All of the previous proposals for invisibility require materials with extreme properties. Here we show that transformation optics of a curved, non-Euclidean space (such as the surface of a virtual sphere) relax these requirements and can lead to invisibility in a broad band of the spectrum.

Geometry has always played a distinguished role in optics (1), but direct optical applications of differential geometry are rather recent (2–4). Most notably, electromagnetic cloaking devices (5) are inspired by ideas of transformation optics (6–10), whereby transparent materials mimic coordinate transformations, forcing light to follow curved coordinates. The coordinates may enclose a hidden space, making the interior invisible and the act of cloaking undetectable. Another application of transformation optics (3, 4) is negative refraction (11, 12), where light follows coordinates that run backward in space (2) or time (13). One can also create optical analogs of the event horizon (2, 3, 14) and perhaps even electromagnetic wormholes (15). The key to engineering practical implementations of ideas that normally belong to general relativity (2–4) is the application of modern metamaterials (16–19). In metamaterials, man-made subwavelength structures generate unusual electromagnetic and optical properties. Metamaterials are potentially very versatile, but they are still subject to fundamental limits.

Take, for instance, the cloaking device (10) with the coordinate transformation illustrated in Fig. 1. The coordinates of physical space (Fig. 1B) are curved transformations of straight Car-

tesian coordinates in a virtual space that we call electromagnetic space (2) (Fig. 1A). This space is empty, so light follows straight lines that appear curved in physical space. If the coordinate transformation expands one point in electromagnetic space to an extended volume in physical space, anything in the “interior of the point” is invisible, as shown in Fig. 1B. However, Fig. 1 also reveals a fundamental problem of such cloaking devices. In electromagnetic space, light passes a point in infinitely short time, but in physical space the point has become an extended region. Thus, light

must propagate along the inner lining of the cloak at infinite speed (2). In materials, including metamaterials, the phase velocity (I) of light may approach infinity, but only at discrete frequencies that correspond to resonances of the material’s constituents. Light with different frequencies (different colors) would not be cloaked but instead be distorted. Furthermore, the group velocity (I) tends to be zero at resonances: Light pulses would become glued to the device instead of traveling around it (20). Therefore, turning invisibility from a tantalizing idea into a practical broadband device requires a different approach.

So far, transformation optics have mostly applied concepts of only Euclidean, flat space, the curved light rays being mere coordinate transformations of a space that is inherently flat. Here we explain how concepts of non-Euclidean geometry (i.e., of intrinsically curved space) could pave the way to broadband invisibility. In curved space, light may propagate along closed loops or may avoid some regions altogether. Most transparent materials act as if they would curve the geometry of light (3); light focused by a lens, refracted in a water droplet, or bent in a mirage perceives space as being curved, in general. Transformation media where the perceived space is inherently flat are the exceptions (3). However, to

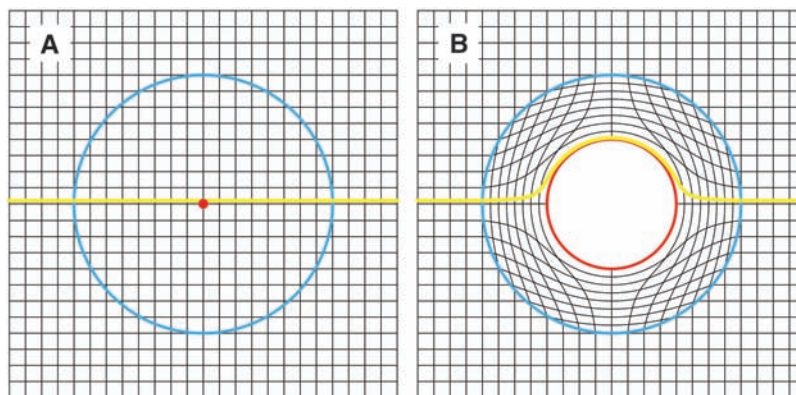


Fig. 1. Euclidean cloaking device (10). The device performs a coordinate transformation from the virtual space (A) to physical space (B). The virtual space is empty and flat (Euclidean). Because the curved coordinate lines of physical space are transformations of straight lines, physical space is Euclidean as well. The device creates the illusion that light propagates through flat space that is empty, apart from one point that, in physical space, has been expanded to finite size. The interior of the expanded point is hidden. Light, however, passes a point in infinitely short time. So, in physical space, the speed of light in the material of the device must approach infinity, which severely limits the use of Euclidean cloaking (10).

¹Physics Department, National University of Singapore, 2 Science Drive 3, Singapore 117542, Singapore. ²School of Physics and Astronomy, University of St. Andrews, North Haugh, St. Andrews, KY16 9SS, UK. ³Institute of Theoretical Physics and Astrophysics, Masaryk University, Kotlarska 2, 61137 Brno, Czech Republic.

*To whom correspondence should be addressed. E-mail: ulf@st-andrews.ac.uk

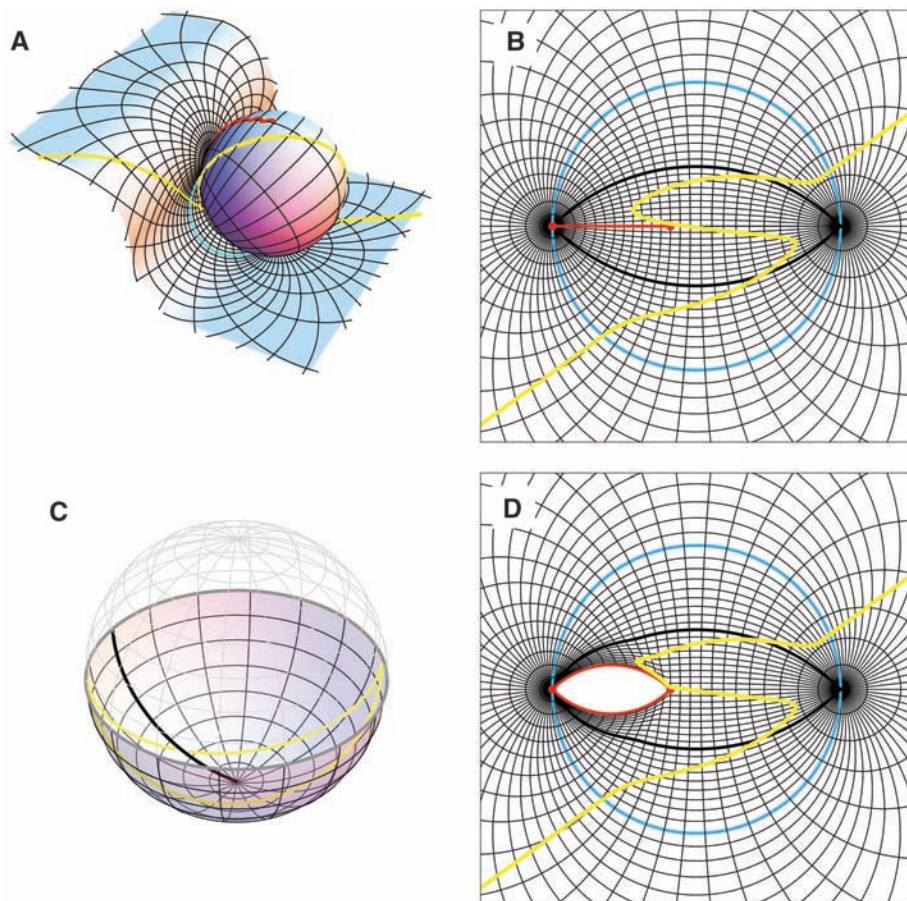


Fig. 2. Non-Euclidean cloaking device in two dimensions. The device creates the illusion shown in (A): Light propagates through a virtual space that consists of a plane and the surface of a sphere, a curved space, which touch along a line. Some incident light rays venture from the plane to the sphere; they return after one loop and continue in the same direction. Note that the rays never cross the red zigzag line on the sphere. Plane and sphere carry a coordinate grid that is mapped onto physical space (B). The magenta circle defines the boundary of the device. Its interior has been expanded to make space for the grid of the sphere. In particular, the line where plane and sphere touch has been opened like an eye (thick black lines) to include the sphere. This is not a cloaking device yet, but one could place a mirror around the equator of the virtual sphere (C), making the northern hemisphere invisible and creating the same illusion as shown in (A). (D) Alternatively, one could expand the red line that light never crosses to create a hidden space.

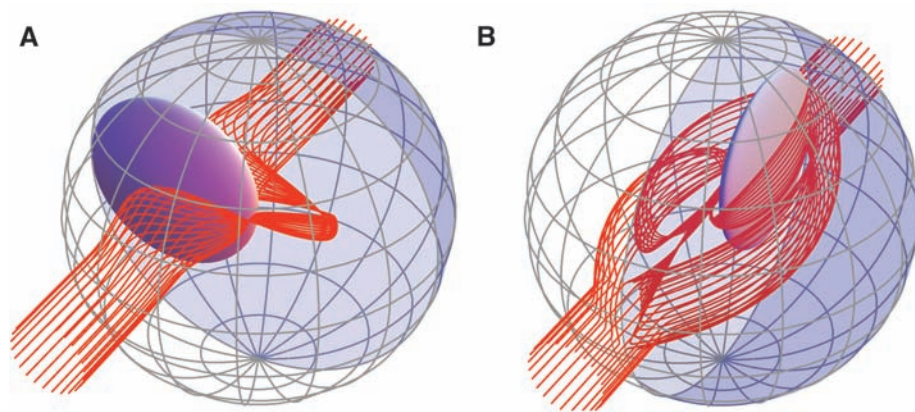


Fig. 3. 3D cloaking. One can extrapolate the ideas illustrated in Fig. 2 to 3D space, replacing the plane by flat space and the sphere by a hypersphere. The lentil-shaped object indicates the hidden interior of the device, and the partly shaded grid denotes the boundary of the invisibility device. For better contrast, light rays are shown in red. (A) Rays are bent around the invisible region. (B) In three dimensions, some rays turn out to perform two loops in hyperspace that appear in physical space as light wrapped around the invisible interior.

achieve invisibility, it is necessary to curve the geometry in specific ways.

We explain our ideas with pictures, the complete calculations behind the pictures being described in the supporting online material (21). As three-dimensional (3D) curved space is difficult to visualize, we first explain our concept on a 2D example and then extend this case to three dimensions. Figure 2A shows the archetype of a non-Euclidean space (the surface of a sphere) combined with a Euclidean space (the plane) that touches the sphere like a piece of paper partially wrapped around a globe. Both the plane and the sphere carry a coordinate grid that we map onto physical space (the plane shown in Fig. 2B). The entrance to the sphere (i.e., the line where the globe touches the plane) has been opened like an eye in the physical plane to make space for the grid of the sphere. In mathematical terminology, electromagnetic space consists of two branches, plane and sphere, that are connected at a branch cut. Although the globe has been flattened in physical space, the exterior curvature of the sphere is maintained as intrinsic curvature.

As there is a one-to-one correspondence between light propagation in the physical plane (Fig. 2B) and in electromagnetic space (Fig. 2A), we discuss the optics in electromagnetic space. Light rays follow geodesics (3), lines of shortest or longest path (1, 3). The geodesics on the sphere are the great circles. Light entering the sphere through the branch cut performs a loop and leaves in the same direction as before; the sphere is invisible but it does not make anything else invisible yet. However, if we place a mirror around the equator of the globe (Fig. 2C), light is reflected twice, creating the illusion of following a great circle, yet never reaching the northern hemisphere. Anything placed inside the corresponding area in physical space is invisible. A more elegant option instead of hiding behind a mirror is the creation of an invisible space that light naturally avoids (22). For example, the light circles on the sphere never cross the red zigzag shown in Fig. 2A. Imagine we open the zigzag like a zip in physical space (Fig. 2D). Anything inside this region is hidden, and the act of hiding is not detectable on the light rays: We have a cloaking device. On the other hand, light performs loops on the sphere, which takes time. Measuring time delays or examining the phase fronts of light rays could reveal the presence of the cloaking device. This imperfection (9, 22) is the price to pay for practical invisibility, whereas perfect invisibility (10) is not practical.

The implementation of our idea does not demand extreme optical properties such as infinities or zeros of the speed of light, for the following reason: In electromagnetic space, light propagates at the speed of light in vacuum. Physical space represents a deformed image of electromagnetic space; the speed of light follows this deformation. Expressed in quantitative terms, if an infinitesimal line element in electromagnetic space is n times longer than its image in physical

space, then the refractive index in the corresponding direction in physical space is n . Figure 2 as well as calculations (21) show that the ratio of the line elements is neither infinite nor zero. Even at a branch point the spatial deformation in any direction is finite, because here the coordinate grid is only compressed in angular direction by a finite factor, in contrast to optical conformal mapping (9). Furthermore, the spatial deformations are gradual, for avoiding reflections at boundaries (23).

Figure 3 illustrates the extension of our idea to three dimensions. Instead of the 2D surface of the globe of Fig. 2A, we use the 3D surface of a 4D sphere (a hypersphere). Such a geometry is realized (24, 25) in Maxwell's fish eye (1, 26). Inside the cloaking device, we inflate a 2D surface, the branch cut in 3D, like a balloon to make space for the 3D surface of the hypersphere. Again, at this point the cloak is invisible but does not hide anything yet. Then we open another spatial branch on the "zip" of the hypersphere to create a hidden interior. The branch cuts are curved surfaces in electromagnetic space, which is the only important difference when compared with the 2D case. Some light rays may pierce the entrance to the hypersphere twice; they perform two loops in the non-Euclidean branch. In physical space, light is wrapped around the invisible interior in such cases (Fig. 3B). We calculated

the required electromagnetic properties (21) and found that the electric permittivity ranges from 0.28 to 31.2 for our specific example. One could give the cloaking device any desired shape by further coordinate transformations, which would change the requirements on the optical properties of the material. As a rule, the larger the cloaked fraction of the total volume of the device, the stronger the optics of the material must be, but the required speed of light will always remain finite.

References and Notes

- M. Born, E. Wolf, *Principles of Optics* (Cambridge Univ. Press, Cambridge, 1999).
- U. Leonhardt, T. G. Philbin, *New J. Phys.* **8**, 247 (2006).
- U. Leonhardt, T. G. Philbin, in press; preprint available at <http://arxiv.org/abs/0805.4778> (2008).
- V. M. Shalaev, *Science* **322**, 384 (2008).
- D. Schurig *et al.*, *Science* **314**, 977 (2006), published online 18 October 2006; 10.1126/science.1133628.
- An early precursor of transformation optics is (7).
- L. S. Dolin, *Izvestiya Vusov* **4**, 964 (1961).
- A. Greenleaf, M. Lassas, G. Uhlmann, *Math. Res. Lett.* **10**, 1 (2003).
- U. Leonhardt, *Science* **312**, 1777 (2006), published online 24 May 2006; 10.1126/science.1126493.
- J. B. Pendry, D. Schurig, D. R. Smith, *Science* **312**, 1780 (2006), published online 24 May 2006; 10.1126/science.1125907.
- J. Yao *et al.*, *Science* **321**, 930 (2008).
- J. Valentine *et al.*, *Nature* **455**, 376 (2008).
- J. B. Pendry, *Science* **322**, 71 (2008), published online 28 August 2008; 10.1126/science.1162087.

- T. G. Philbin *et al.*, *Science* **319**, 1367 (2008).
- A. Greenleaf, Y. Kurylev, M. Lassas, G. Uhlmann, *Phys. Rev. Lett.* **99**, 183901 (2007).
- G. W. Milton, *The Theory of Composites* (Cambridge Univ. Press, Cambridge, 2002).
- D. R. Smith, J. B. Pendry, M. C. K. Wiltshire, *Science* **305**, 788 (2004).
- C. M. Soukoulis, S. Linden, M. Wegener, *Science* **315**, 47 (2007).
- A. K. Sarychev, V. M. Shalaev, *Electrodynamics of Metamaterials* (World Scientific, Singapore, 2007).
- H. Chen, C. T. Chan, *J. Appl. Phys.* **104**, 033113 (2008).
- See the supporting material on *Science* Online.
- U. Leonhardt, *New J. Phys.* **8**, 118 (2006).
- W. S. Cai, U. K. Chettiar, A. V. Kildishev, V. M. Shalaev, G. W. Milton, *Appl. Phys. Lett.* **91**, 111105 (2007).
- R. K. Luneburg, *Mathematical Theory of Optics* (Univ. of California Press, Berkeley, CA, 1964).
- H. A. Buchdahl, *Am. J. Phys.* **46**, 840 (1978).
- J. C. Maxwell, *Cambridge Dublin Math. J.* **8**, 188 (1854).
- We thank N. V. Korolkova for her generous support of this work. We are grateful for funding from European Union Contract Computing with Mesoscopic Photonic and Atomic States, the grants MSM0021622409 and MSM0021622419, and a Royal Society Wolfson Research Merit Award.

Supporting Online Material

www.sciencemag.org/cgi/content/full/1166332/DC1

SOM Text

Figs. S1 to S15

References

23 September 2008; accepted 5 November 2008

Published online 20 November 2008;

10.1126/science.1166332

Include this information when citing this paper.

Control of Self-Assembly of DNA Tubules Through Integration of Gold Nanoparticles

Jaswinder Sharma,^{1,2*} Rahul Chhabra,^{1,2*} Anchi Cheng,³ Jonathan Brownell,³ Yan Liu,^{1,2†} Hao Yan^{1,2†}

The assembly of nanoparticles into three-dimensional (3D) architectures could allow for greater control of the interactions between these particles or with molecules. DNA tubes are known to form through either self-association of multi-helix DNA bundle structures or closing up of 2D DNA tile lattices. By the attachment of single-stranded DNA to gold nanoparticles, nanotubes of various 3D architectures can form, ranging in shape from stacked rings to single spirals, double spirals, and nested spirals. The nanoparticles are active elements that control the preference for specific tube conformations through size-dependent steric repulsion effects. For example, we can control the tube assembly to favor stacked-ring structures using 10-nanometer gold nanoparticles. Electron tomography revealed a left-handed chirality in the spiral tubes, double-wall tube features, and conformational transitions between tubes.

Nanoparticles can exhibit distinctive electronic, magnetic, and photonic properties (1), and their assembly into well-defined

one-dimensional (1D), 2D, and 3D architectures with geometric controls could add to their functionality. DNA-mediated assembly of nanoparticles is an attractive way to organize both metallic and semiconducting nanoparticles into periodic or discrete 1D and 2D structures (1–14) through the programmable base-pairing interactions and the ability to construct branched DNA nanostructures of various geometries. Recent success in using DNA as a molecular glue to direct gold nanoparticles (AuNPs) into periodic 3D crystalline lattices further demonstrates the

power of DNA as building blocks for 3D nano-engineering (15, 16).

Here, we report a group of complex 3D geometric architectures of AuNPs created using DNA tile-mediated self-assembly. These are tubular nanostructures with various conformations and chiralities resembling those of carbon nanotubes. The nanoparticle tube assembly can be engineered both by the underlying DNA tile scaffolds and the nanoparticles themselves. Previous work in structural DNA nanotechnology has shown that DNA tubes can form through either the self-association of multi-helix DNA bundle structures or the closing up of 2D DNA tile lattices (17–26). The forces that drive tube formation have been attributed to the intrinsic curvature of the tile-array (21) and the thermodynamic requirement to lower the free energy of the system by minimizing the number of unpaired sticky ends (22). The intrinsic dimensional anisotropy of the DNA tiles also plays an important role in the kinetic control of the tube growth (26).

In all of the above studies, the true 3D conformations of DNA tubes have never been revealed in detail because of limitations in microscopic imaging techniques; deposition of the samples on a surface for atomic force microscope (AFM) or transmission electron microscope (TEM) imaging usually causes flattening and sometimes opening of the tubes. This limitation has prevented a comprehensive understanding of the structural features of DNA nanotubes. For example, the handedness of the chiral tubes can be better revealed with 3D structural characteriza-

¹Center for Single Molecule Biophysics, The Biodesign Institute, Arizona State University, Tempe, AZ 85287, USA.

²Department of Chemistry and Biochemistry, Arizona State University, Tempe, AZ 85287, USA. ³National Resource for Automated Molecular Microscopy, The Scripps Research Institute, La Jolla, CA 92037, USA.

*These authors contributed equally to this work.

†To whom correspondence should be addressed. E-mail: hao.yan@asu.edu (H.Y.); yan_liu@asu.edu (Y.L.)